Extended Abstracts of the 21st Conference on Solid State Devices and Materials, Tokyo, 1989, pp. 293-296

D-4-2

Quest for Higher Performance HBTs, AlInAs/GaInAs vs. InP/GaInAs: Monte Carlo Study

Riichi Katoh and Mamoru Kurata

Research and Development Center, Toshiba Corporation

1 Komukai Toshiba-cho, Saiwai-ku
Kawasaki-shi 210, Japan

The high speed performances of AlInAs/GaInAs and InP/GaInAs HBTs were investigated using a self-consistent particle simulator. The cutoff frequencies were estimated to be twice for the former and 1.5 times for the latter as high as that for as AlGaAs/GaAs HBT. These results were attributed to a larger bandgap difference between the emitter and base to yield a high base built-in field, rather than a larger Γ-L band separation energy in the collector layer.

1. Introduction

AlInAs/GaInAs and InP/GaInAs HBTs are considered to be promising devices for their capability of lower power and higher speed operation compared with AlGaAs/GaAs HBTs. Recently reported excellent data for these devices have already revealed their high potentiality as high speed devices, although their research and development periods have been by far the shorter than that of AlGaAs/GaAs HBTs[1),2)]. However, the effects of large Γ-L band separation energy $\Delta E_{\Gamma-L}$ and the base bandgap grading on nonequilibrium electron transport, as well as high speed performance have been left unclear so far.

In this work, these HBTs were compared with each other by particle simulation to clarify these problems in view of high frequency performance.

2. Model

A previously developed one-dimensional particle simulator[3)] was applied to analyze AlInAs/GaInAs and InP/GaInAs HBTs with several modifications in the physical parameters and formulation of random alloy scattering. Bandgap, electron affinity, effective mass, dielectric constant, and other various physical parameters in the scattering rates were determined by the linear interpolation of binary alloy data[4)] to match the lattice constant of the InP substrate. The formulation of the random alloy scattering by Littlejohn, et al.[5)], was adopted for the quaternary alloy systems, i.e., AlGaInAs and GaInAsP.

Figure 1 shows the computed alloy

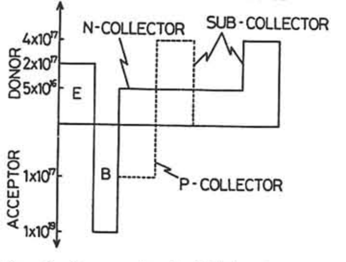

Fig.1 Computed HBT structures

composition and doping profiles, where the fractional variation in material constants is expressed as $(Al_{\alpha}Ga_{1-\alpha})_{0.47}In_{0.53}As$ and $Ga_{0.47(1-\beta)}In_{0.53+0.47\beta}As_{1-\beta}P_{\beta}$. AlInAs/GaInAs HBT and InP/GaInAs HBT will be hereafter referred to as Tr.1 and Tr.2, respectively. A common α profile was applied both for n and p collectors with Tr.1, while different β profiles for n and p collectors with Tr.2. A graded base structure was adopted in order to reduce the base transit time, which was effective even in a heavily doped base layer[3]. Demonstrated profiles for α and β were optimized data, whose derivations will be discussed in the following section. The doping profile was common for Tr.1 and Tr.2, where an n collector with $5x10^{16}cm^{-3}$ in doping and 5000A in length and a p collector with $1x10^{17}cm^{-3}$ and 1500A were considered.

As for the bias condition, the collector-to-emitter voltage V_{CE} was fixed at 1.5V throughout the paper. Every computation was carried out under 300K operation temperature.

3.Computational Results

The alloy compositions α and β at the emitter-base(E-B) junctions were first optimized from the standpoint of a trade off between the emitter charging time τ_E and the base transit time τ_B[3]. Figures 2(a) and 2(b) show the dependence of ($\tau_E + \tau_B$) on compositions α and β at the E-B junctions, respectively, where transit times were defined by $\tau_E = \Delta Q_E / \Delta J_C$ and $\tau_B = \Delta Q_B / \Delta J_C$ at around $J_C = 1x10^5 A/cm^2$. It should be noted that τ_E was obtained from the conventional drift-diffusion model, and τ_B from the particle model. τ_B is seen to decrease monotonically as α and β increase, because of the enhancement of velocity overshoot corresponding to the increase in built-in field strength. On the other hand, τ_E increses as α and β increase, because of the increase in emitter capacitance corresponding to the increase in the turn-on voltage. Consequently, there exist minimums in ($\tau_E + \tau_B$) at around $\alpha = \beta = 0.5$ for both transistors. In Tr.1, τ_B seems to increase at $\alpha \geqq 0.75$. This is attributed to the reduction in electron velocity due to the upper valley transition.

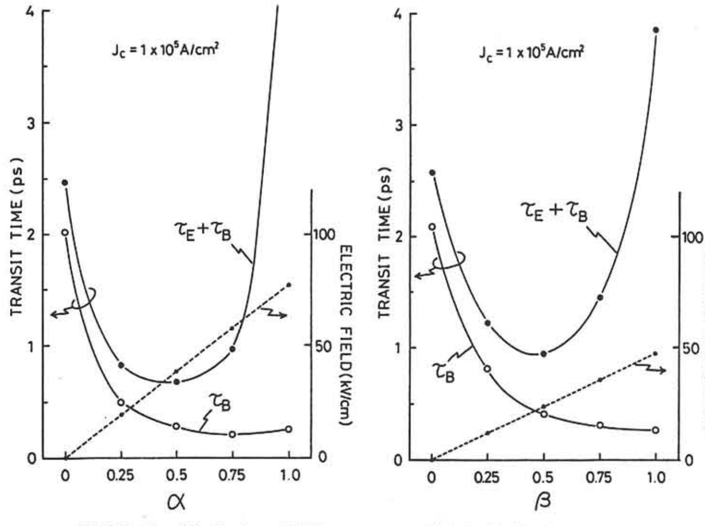

a)AlInAs/GaInAs HBT (b)InP/GaInAs HBT

Fig.2 Alloy composition dependence of emitter charging time and base transit time

Hereafter, $\alpha = \beta = 0.5$ will be chosen at emitter-base junction to minimize ($\tau_E + \tau_B$). Under this condition, the τ_B =0.29ps obtained for Tr.1 and 0.41ps for Tr.2 are 1/3 and 2/5 of τ_B for AlGaAs/GaAs HBTs,

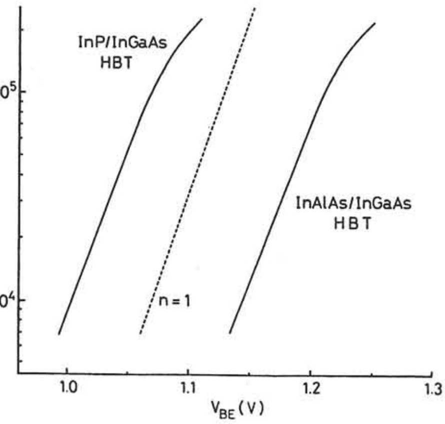

Fig.3 J_C vs. V_{BE} characteristics

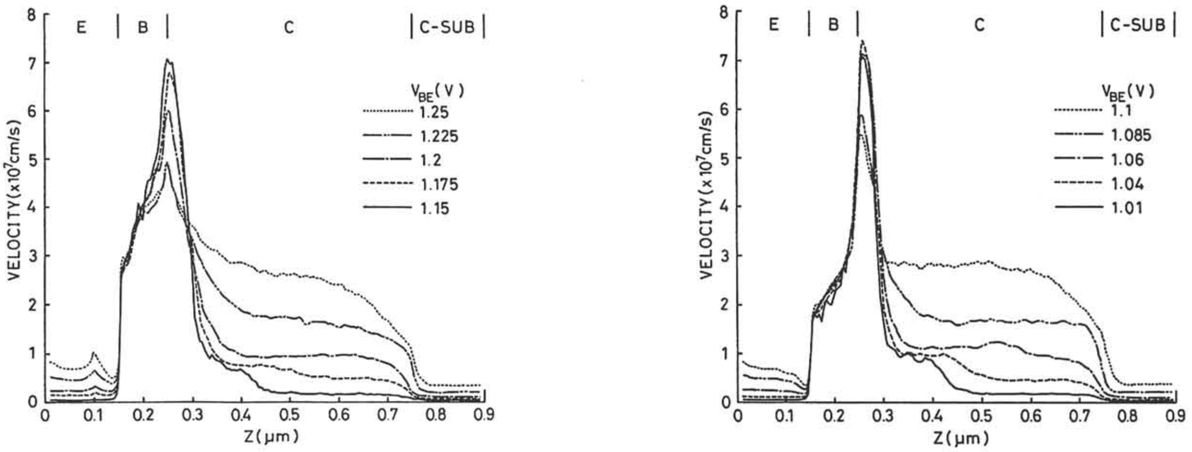

(a)AlInAs/GaInAs HBT (b)InP/GaIAs HBT

Fig.4 Average electron velocity profiles for n collector HBTs

respectively. It should be noted that these small τ_B s are obtained as a consequence of the large bandgap difference between the emitter and base layers.

Figure 3 shows the J_C vs. V_{BE} characteristic for the above optimized HBTs. There was a significant difference in the turn-on voltage (V_{on}) of about 0.14V between Tr.1 and Tr.2. It is noteworthy that V_{on} for Tr.2 was similar to that of Si bipolar transistors.

Figures 4(a) and 4(b) show average electron velocity (V_d) profiles for Tr.1 and Tr.2 with an n collector, respectively, with base-to-emitter voltage(V_{BE}) as a parameter. In the base regions, v_d for Tr.1 was about 1.5 times as large as that for Tr.2, resulting in a smaller τ_B for Tr.1. In the collector regions, the peak overshoot velocity for Tr.2 was a little larger than that for Tr.1, because of the smaller velocity for Tr.2 in the base region$^{3)}$. The overshoot distance was about 750A for both HBTs, which was a little larger than that for GaAs. The saturation velocity(V_s) for Tr.1 is $6x10^6$ cm/s and that for Tr.2 was $1x10^7$ cm/s. The small V_s of Tr.1 is attributed to its larger effective mass due to a strong nonparabolicity. At a larger V_{BE}, V_d of both HBTs began to increase in a wider range of the collector region, thus decreasing the collector transit time τ_C. This phenomenon is attributed to the relaxation of the electeric field at the onset of the collector high injection effect (Kirk efect) $^{3),6)}$. Though the peak overshoot velocity decreased markedly as V_{BE} increased, it was insensitive to the magnitude of τ_C since the overshoot velocity was inherently large.

Figures 5(a) and 5(b) show V_d profiles for Tr.1 and Tr.2 with a p collector, respectively, with V_{BE} as a parameter. Compared with the n collector cases, the difference between Tr.1 and Tr.2 seems to be very slight. The peak overshoot velocity and the overshoot distance for Tr.1 were a little larger than those for Tr.2, which was

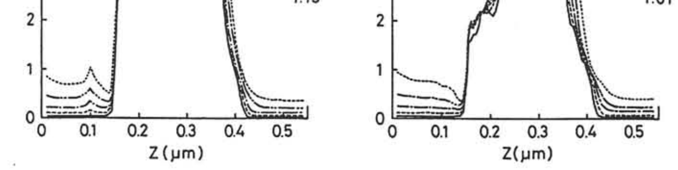

(a)AlInAs/GaInAs HBT (b)InP/GaInAs HBT

Fig.5 Average electron velocity profiles for p collector HBTs

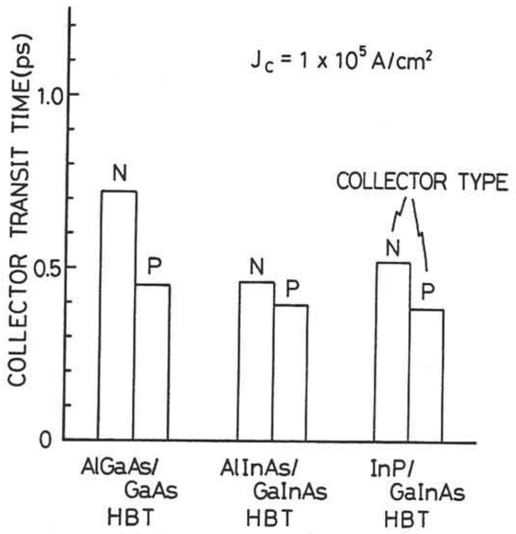

fog.6 Collector structure dependence of collector transit times

due to the larger $\Delta E_{\Gamma\text{-}L}$ of Tr.1.

Figure 6 shows τ_Cs for Tr.1 and Tr.2 with n and p collectors, with corresponding data for AlGaAs/GaAs HBT. With n collector HBTs, Tr.1 exhibited the smallest τ_C, while the difference between Tr.1 and Tr.2 was only less than 0.1ps. Since τ_C for an n collector transistor decreased under a high injection condition of the upper half of 10^4 A/cm^2, τ_C became sensitive to the bias condition. In this case, however, smaller τ_Cs for Tr.1 and Tr.2 compared with the GaAs transistor were considered to be a consequence of a larger $\Delta E_{\Gamma\text{-}L}$. Contrary to the n collector cases, little difference was observed in the τ_Cs for p collectors. This is because the high average electron velocity has already been achieved by introducing a p collector structure.

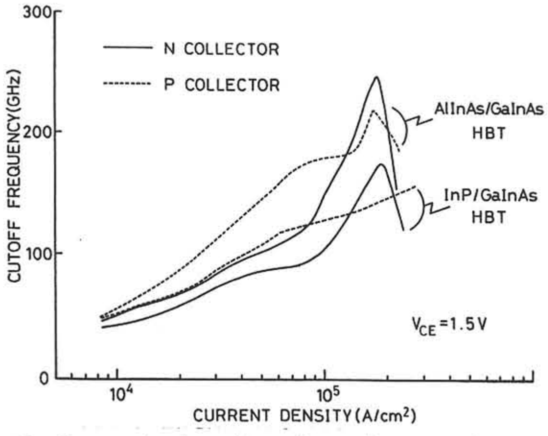

Fig.7 Current density dependence of cutoff frequency

In order to investigate the high speed performance of these HBTs, the cutoff frequency (f_T) vs. current density(J_C) characteristic are demonstrated for Tr.1 and Tr.2 with n and p collectors in Fig.7. At J_C of less than 10^5 A/cm^2, p collector HBTs exhibited higher f_T than n collector HBTs. On the other hand, under a higher J_C condition, f_T for n collector HBTs became higher than those for p collector HBTs. The maximum f_Ts are 250GHz and 220GHz for Tr.1 with n and p collectors, and 180GHz and 160GHz for Tr.2 with n and p collectors, respectively. Therefore, Tr.1 and Tr.2 were twice and 1.5 times as fast as GaAs HBTs, respectively.

4.Conclusions

The cutoff frequencies of AlInAs/GaInAs and InP/GaInAs HBTs were estimated to be twice and 1.5 times as high as that of AlGaAs/GaAs HBT, respectively, thus verifying their promising high speed performance. The main reason for the improved high speed operation is attributed to the larger bandgap ratio between the emitter and base, which yields a high base built-in field, rather than the larger Γ-L band separation energy.

References

1)U.K.Mishra et al.,IEDM Tech.Dig.(1988)873.
2)Y-K.Chen et al.,IEEE Elect.Dev.Lett., 10(1989)267.
3)R.Katoh et al.,IEEE Trans.on Elect.Dev.,ED-36(5) (1989)846.
4)S.Adachi,J.Appl.Phys.,53(12)(1982)8775.
5)M.A.Littlejohn et al.,Solid State Electron.,21(1978)107.
6)R.Katoh et al.,to be published in Trans.on Elect.Dev., ED-36(10) (1989).